



The ultra-high energy cosmic ray spectrum and Fermi shock acceleration

M. KACHELRIESS¹, D.V. SEMIKOZ^(2,3)

¹*Institutt for fysikk, NTNU, N-7491 Trondheim, Norway*

²*APC, 10 rue Alice Domon and Leonie Duquet, Paris 75205, France*

³*INR RAS, 60th October Anniversary prospect 7a, 117312 Moscow, Russia*

e-mail: dmitri.semikoz@apc.univ-paris7.fr

Abstract: The energy spectrum of ultra-high energy cosmic rays (UHECR) is usually calculated for sources with identical properties. Assuming that all sources can accelerate UHECR protons to the same extremely high maximal energy $E_{max} > 10^{20}$ eV and have the steeply falling injection spectrum $1/E^{2.7}$, one can reproduce the measured cosmic ray flux above $E > 10^{18}$ eV. In our paper [1] we have shown that relaxing the assumption of identical sources and using a power-law distribution of their maximal energy allows one to explain the observed UHECR spectrum with the injection $1/E^2$ predicted by Fermi shock acceleration.

Introduction

The UHECR proton spectrum should be strongly suppressed above $E \gtrsim 5 \times 10^{19}$ eV due to pion production on cosmic microwave photons, the so called Greisen-Zatsepin-Kuzmin (GZK) cutoff [2]. Another signature for extragalactic protons is a dip (or ankle) in the CR flux around 5×10^{18} eV seen in the experimental data of AGASA, Fly's Eye, HiRes and Yakutsk.

Several groups of authors have tried previously to explain the observed spectral shape of UHECR flux using mainly two different approaches: In the first one, the ankle is identified with the transition from a steep galactic, usually iron-dominated component to an extragalactic one with injection spectrum between $\sim 1/E^2$ and $1/E^{2.3}$. The latter component was chosen either as proton dominated [3] or, more recently, with a mixed composition [4]. In the second approach, the dip is a feature of e^+e^- pair production and one is able to fit the UHECR spectrum down to $E \sim 10^{18}$ eV using only extragalactic protons and an injection spectrum between $1/E^{2.6}$ and $1/E^{2.7}$ [5]. Chemical composition studies [6, 7] of the CR flux of both the AGASA [8] and HiRes [9] experiments point to the dominance of protons above 10^{18} eV, while Fly's Eye data show a transition in the ankle region [10].

These results depend however strongly on the details of the used hadronic interaction models. Both improvements of these models and of the measuring accuracy are needed to answer this question in the future.

A basic ingredient of previous analyzes is the assumption that the sources are identical. In particular, it is assumed that every source can accelerate protons to the same maximal energy E_{max} , typically chosen as 10^{21} eV or higher. However, one expects that E_{max} differs among the sources and that the number of potential sources becomes smaller and smaller for larger E_{max} . Therefore two natural questions to ask are i) can one explain the observed CR spectrum with non-identical sources? And ii), is in this case a good fit of the CR spectrum possible with a power-law and exponent $\alpha \sim 2$ as predicted by Fermi shock acceleration?

In Ref. [1] we addressed these two questions and show that choosing a power-law distribution $dn/dE_{max} \propto E_{max}^{-\beta}$ for E_{max} allows one to explain the measured energy spectrum e.g. for $\alpha = 2$ with $\beta = 1.7$.

Fitting the AGASA and HIRES data

We assume a continuous distribution of CR sources with constant comoving density up to the maximal redshift $z_{\max} = 2$. Then UHECRs are generated according to the injection spectrum

$$\frac{dN}{dE} \propto E^{-\alpha} \vartheta(E_{\max} - E), \quad (1)$$

and are propagated until their energy is below 10^{18} eV or they reach the Earth. The proton propagation was simulated with the Monte Carlo code of Ref. [11]. The maximal energy E_{\max} in Eq. (1) is chosen as $E_{\max} = 10^{21}$ eV.

The use of a power-law for the injection spectrum of UHECRs is well-motivated by models of shock acceleration [12]. However, these models predict as exponent typically $\alpha \approx 2.0$ – 2.2 . Moreover, the maximal acceleration energy of a certain source depends obviously on parameters that vary from source to source like its magnetic field strength or its size [13, 14]. Therefore, one expects that E_{\max} varies vastly among different sources with less and less sources able to accelerate cosmic rays to the high-energy end of the spectrum.

Here we relax the assumption of identical sources and suggest to use a power-law distribution for the maximal energies of the individual sources,

$$\frac{dn}{dE_{\max}} \propto E_{\max}^{-\beta}. \quad (2)$$

Without concrete models for the sources of UHECRs, we cannot derive the exact form of the distribution of E_{\max} values. However, the use of a power-law for the E_{\max} distribution is strongly motivated by the following two reasons: First, we expect a monotonically decreasing distribution of E_{\max} values and, for the limited range of two energy decades we consider, a power-law distribution should be a good approximation to reality. Second, the use of a power-law distribution for E_{\max} with exponent

$$\beta = \alpha + 1 - \alpha_0, \quad (3)$$

guaranties to recover the spectra calculated with Eq. (1), i.e. $E_{\max} = \text{const.}$, for the special case of $E_{\max} \rightarrow \infty$ and a continuous distribution of sources. For finite values of E_{\max} and the source density n_s , the effective injection spectrum is not

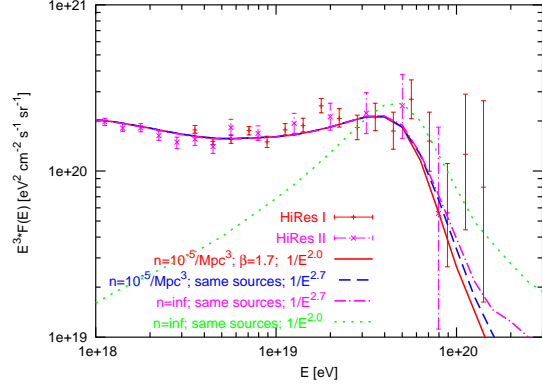


Figure 1: Fits of the HiRes I and HiRes II data are shown for a uniform distribution of identical sources with power-law injection spectrum $1/E^2$ (green, dashed line) and $1/E^{2.7}$ (magenta, dash-dotted line) for an infinite number of sources as well as for a realistic source density $n_s = 10^{-5}/\text{Mpc}^3$ and spectrum $1/E^{2.7}$ (blue, dashed line). The case of an $1/E^2$ spectrum and maximal energy dependence from Eq. (2) with $\beta = 1.7$ is shown as a red, solid line.

described anymore by a single power-law. However, deviations show-up only at energies above $\approx 6 \times 10^{19}$ eV or small source densities, see below.

The results for 5.000 Monte Carlo runs of our simulation are presented in Fig. 1 for HiRes [9] and in Fig. 2 for Akeno/AGASA. In order to combine the AGASA [8] with the Akeno [15] data in Fig. 2, we have rescaled systematically the AGASA data 10% downwards. In the standard picture of uniform sources with identical maximal energy (here, $E_{\max} = 10^{21}$ eV) and $1/E^2$ spectrum, extragalactic sources contribute only to a few bins of the spectrum around the GZK cutoff, cf. the green-dotted line in Fig. 1. By contrast, an injection spectrum $1/E^{2.7}$ allows one to explain the observed data down to $\approx 10^{18}$ eV with extragalactic protons from identical sources, cf. the magenta, dash-dotted line for a continuous and the blue, dashed line for a finite source distribution with $n_s = 10^{-5}/\text{Mpc}^3$ in Fig. 1. This well-known result can be obtained also for an injection spectrum $1/E^2$ of individual sources, if for the E_{\max} distribution, Eq. (2), the exponent $\beta = 1.7$ is

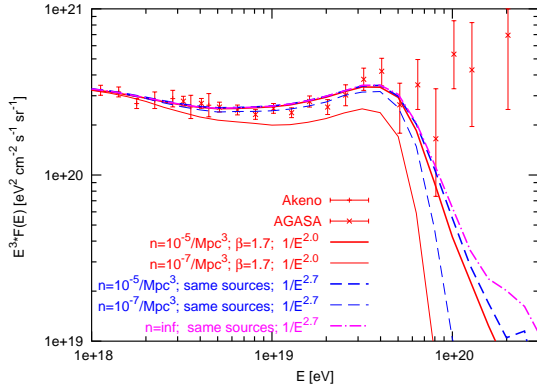


Figure 2: The fit of Akeno/AGASA data using a uniform distribution of identical sources for an infinite number of sources and power-law spectrum $1/E^{2.7}$ is shown as a magenta, dash-dotted line. The same fit with the realistic source density $n_s = 10^{-5}/\text{Mpc}^3$ and spectrum $1/E^{2.7}$ (thick blue dashed line) and $1/E^2$ spectrum and maximal energy dependence from Eq. (2) with $\beta = 1.7$ is shown as a thick red, solid line. The thin red, solid line for the spectrum $1/E^2$ and $\beta = 1.7$ and the thin blue, dashed line for the spectrum $1/E^{2.7}$ correspond to the low source density $n_s = 10^{-7}/\text{Mpc}^3$.

chosen. This is illustrated by the red, solid line in Fig. 1 for the case of a finite source density $n_s = 10^{-5}/\text{Mpc}^3$.

In Fig. 2, we show the dependence of our results on the source density n_s together with the Akeno/AGASA data. While for large enough source densities, $n_s = 10^{-5}/\text{Mpc}^3$, the spectra from identical sources with $1/E^{2.7}$ and from sources with $1/E^2$ injection spectrum, variable E_{max} and $\beta = 1.7$ are very similar, for smaller densities, $n = 10^{-7}/\text{Mpc}^3$ in Fig. 2, the shape of the spectra differs considerably even at lower energies. Thus for small source densities the relation (3) is not valid anymore.

From our results presented in Figs. 1 and 2, we conclude that the power-law injection spectrum $1/E^{2.7}$ found earlier may be seen as the combined effect of an injection spectrum $1/E^2$ predicted by Fermi acceleration and a power-law distribution of the maximal energies of individual sources with

$\beta = 1.7$, if the source density is sufficiently large, $n_s \gtrsim 10^{-5}/\text{Mpc}^3$. More generally, the exponent α_0 obtained from fits assuming identical sources is connected simply by Eq. (3) to the parameters α and β determining the power-laws of variable sources in this regime.

Discussion

The minimal model we proposed can explain the observed UHECR spectrum for $E > 10^{18}$ eV with an injection spectrum as predicted by Fermi acceleration mechanism, $\alpha = 2-2.2$. However, in general the experimental data can be fitted for any value of α in the range $2 \leq \alpha \leq 2.7$ by choosing an appropriate index $\beta = \alpha + 1 - \alpha_0$ in Eq. (2). The best-fit injection spectrum with $\alpha = 2.7$ found for $E_{\text{max}} = \text{const.}$ appears in our model as an effective value that takes into account the averaging over the distribution of E_{max} values for various sources.

For completeness, we consider now the case of sources with variable luminosity. The total source luminosity can be defined by

$$L(z) = L_0(1+z)^m \vartheta(z_{\text{max}} - z) \vartheta(z - z_{\text{min}}), \quad (4)$$

where m parametrizes the luminosity evolution, and z_{min} and z_{max} are the redshifts of the closest and most distant sources. Sources in the range $2 < z < z_{\text{max}}$ have a negligible contribution to the UHECR flux above 10^{18} eV. The value of z_{min} is connected to the density of sources and influences strongly the shape of bump and the strength of the GZK suppression [11, 21].

The value of m influences the spectrum in the range 10^{18} eV $< E < 10^{19}$ eV [5], but less strongly than the parameter β from Eq. (2). Positive values of m increase the contribution of high-redshift sources and, as a result, injection spectra with $\alpha < 2.7$ can fit the observed data even in the case of the same E_{max} for all sources. For example, $\alpha = 2.6$ and $m = 3$ fits the AGASA and HiRes data as well as $\alpha = 2.7$ and $m = 0$ ($\chi^2/\text{d.o.f.} < 1$). However, a good fit with $\alpha = 2$ requires a unrealistic strong redshift evolution of the sources, $m = 16$.

We have presented fits of our model only to the data of Akeno/AGASA and HiRes. In the future, data of the Pierre Auger Observatory [22] and

the Telescope Array [23] will restrict the parameter space of theoretical models similar to one presented here. If a clustered component or even individual sources can be identified in the future data, their spectra will allow one to distinguish between different possibilities for the injection spectrum. Intriguingly, the energy spectrum of the clustered component found by the AGASA experiment is much steeper than the overall spectrum [24]. Thus, one might speculate this steeper spectrum is the first evidence for the "true" injection spectrum of UHECR sources.

References

- [1] M. Kachelriess and D. V. Semikoz, Phys. Lett. B **634**, 143 (2006) [arXiv:astro-ph/0510188].
- [2] K. Greisen, Phys. Rev. Lett. **16**, 748 (1966); G. T. Zatsepin and V. A. Kuzmin, JETP Lett. **4**, 78 (1966) [Pisma Zh. Eksp. Teor. Fiz. **4**, 114 (1966)].
- [3] C. T. Hill, D. N. Schramm and T. P. Walker, Phys. Rev. D **34**, 1622 (1986).
- [4] D. Allard, E. Parizot and A. V. Olinto, Astropart. Phys. **27**, 61 (2007) [arXiv:astro-ph/0512345].
- [5] V. Berezhinsky, A. Z. Gazizov and S. I. Grigorieva, hep-ph/0204357; astro-ph/0210095; Nucl. Phys. Proc. Suppl. **136**, 147 (2004) [astro-ph/0410650]; Phys. Lett. B **612** (2005) 147 [astro-ph/0502550].
- [6] K. Shinozaki *et al.*, Proc. 28th ICRC (Tsukuba), **1**, 437 (2003).
- [7] D. R. Bergman *et al.*, Proc. 29th ICRC (Pune), 2005 [astro-ph/0507483].
- [8] M. Takeda *et al.*, Astropart. Phys. **19**, 447 (2003) [astro-ph/0209422].
- [9] R. U. Abbasi *et al.*, Phys. Rev. Lett. **92**, 151101 (2004) [astro-ph/0208243]; D. R. Bergman [the HiRes Collaboration], astro-ph/0507484.
- [10] D. Bird *et al.*, Phys. Rev. Lett. **71**, 3401 (1993).
- [11] M. Kachelrieß and D. Semikoz, Astropart. Phys. **23**, 486 (2005) [astro-ph/0405258].
- [12] V. S. Berezhinskii *et al.*, Astrophysics of cosmic rays, Amsterdam: North-Holland 1990. T. Gaisser, Cosmic Rays and Particle Physics, Cambridge University Press 1991.
- [13] R. J. Protheroe and R. W. Clay, Publ. Astron. Soc. of Australia **21**, 1 (2004) [astro-ph/0311466].
- [14] R. J. Protheroe, Astropart. Phys. **21**, 415 (2004) [astro-ph/0401523].
- [15] M. Nagano *et al.*, J. Phys. **G10**, 1295 (1984).
- [16] D. De Marco, P. Blasi and A. V. Olinto, Astropart. Phys. **20**, 53 (2003) [astro-ph/0301497].
- [17] M. Lemoine, Phys. Rev. D **71**, 083007 (2005) [astro-ph/0411173].
- [18] F. W. Stecker and S. T. Scully, Astropart. Phys. **23**, 203 (2005) [astro-ph/0412495].
- [19] M. Kachelrieß, P. D. Serpico and M. Teshima, astro-ph/0510444.
- [20] V. Berezhinsky, astro-ph/0509069.
- [21] M. Kachelrieß, D. V. Semikoz and M. A. Tortola, Phys. Rev. D **68** (2003) 043005 [hep-ph/0302161]; P. Blasi and D. De Marco, Astropart. Phys. **20** (2004) 559 [astro-ph/0307067].
- [22] P. Sommers *et al.* [Pierre Auger Collaboration], astro-ph/0507150.
- [23] M. Fukushima, Prog. Theor. Phys. Suppl. **151** (2003) 206.
- [24] M. Takeda *et al.*, Proc. 27th ICRC (Hamburg), **1**, 341 (2001).